



Bioinformatics analysis of immune infiltrates and tripartite motif (*TRIM*) family genes in hepatocellular carcinoma

Jun Cao^{1#}, Bingbing Su^{1#}, Rui Peng^{1#}, Hao Tang¹, Daoyuan Tu¹, Yuhong Tang¹, Jie Zhou¹, Guoqing Jiang¹, Shengjie Jin¹, Qian Wang¹, Aoqing Wang¹, Renjie Liu¹, Qiangwei Deng², Chi Zhang^{1,3}, Dousheng Bai^{1,3}

¹Department of Hepatobiliary Surgery, Clinical Medical College, Yangzhou University, Yangzhou, China; ²Chenzhou municipal Hospital of Chinese Medicine, Chenzhou, China; ³General Surgery Institute of Yangzhou, Yangzhou University, Yangzhou, China

Contributions: (I) Conception and design: D Bai, C Zhang, J Cao, B Su, R Peng; (II) Administrative support: D Bai, C Zhang; (III) Provision of study materials or patients: J Cao, B Su, R Peng, H Tang, D Tu, Y Tang, J Zhou; (IV) Collection and assembly of data: S Jin, R Liu, G Jiang, Q Wang, A Wang, Q Deng; (V) Data analysis and interpretation: J Cao, B Su; (VI) Manuscript writing: All authors; (VII) Final approval of manuscript: All authors.

[#]These authors contributed equally to this work and should be considered as co-first authors.

Correspondence to: Dousheng Bai; Chi Zhang. Department of Hepatobiliary Surgery, Clinical Medical College, Yangzhou University, 98 West Nantong Rd, Yangzhou 225000, China. Email: drbaidousheng@yzu.edu.cn; 18051062769@yzu.edu.cn.

Background: The tripartite motif (*TRIM*) family are important members of the Gene-finger-containing E3 ubiquitin-conjugating enzyme and are involved in the progression of hepatocellular carcinoma (HCC). Previous studies have largely focused on gene expression and molecular pathways, while the underlying role of the *TRIM* family in the tumor immune microenvironment (TIME) remains poorly understood.

Methods: We systematically explored the correlations of prominent *TRIM* genes with immune checkpoints and immune infiltrates in 231 HCC samples [International Cancer Genome Consortium (ICGC) cohort (n=231); The Cancer Genome Atlas (TCGA) cohort (n=370)]. A prognostic risk model was constructed using the least absolute shrinkage and selection operator (LASSO) algorithm and multivariate Cox regression analysis in the ICGC cohort. Kaplan-Meier curves based on the overall survival (OS) were used to assess differences in survival between clusters. We utilized gene set variation analysis (GSVA) to characterize the differences in biological functions. Based on univariate and multivariate Cox progression analysis, we developed a risk score signature and verified its reliability and validity. The Tumor Immune Single-cell Hub (TISCH) single-cell database was employed to evaluate the correlation of *TRIM* genes with the tumor microenvironment.

Results: Cluster 1 was preferentially associated with a favorable prognosis (P<0.001). The amino acid, fatty acid, and drug metabolism pathways were significantly enriched in cluster 2. A prognosis risk score project was established and evaluated based on the 9 independent prognostic genes (all P<0.05). The immune score and stromal scores of patients with low-risk scores were greater than those of patients with high-risk scores (all P<0.001). However, patients with a high-risk score exhibited lower responses to immune checkpoint inhibitors (ICIs), sorafenib, and transarterial chemoembolization (TACE) treatment (all P<0.05). Consistently, *TRIM* genes showed the same influence in the external TCGA cohort. *TRIM* gene-based signatures were implicated in TIME and their copy-number alterations dynamically impacted the abundance of tumor-infiltrating immune cells.

Conclusions: Our findings revealed that MID1, TRIM5, TRIM22, TRIM28, TRIM 31, TRIM37, TRIM38, TRIM47, and TRIM74 could serve as efficient prognostic biomarkers and therapeutic targets in HCC. The identified *TRIM* gene-based signatures could serve as important TIME mediators in HCC, potentially increasing immune treatment efficacy.

Keywords: Hepatocellular carcinoma (HCC); tripartite motif (*TRIM*) genes; tumor immune microenvironment (TIME); immune infiltrates; immunotherapy

Submitted Jul 05, 2022. Accepted for publication Aug 05, 2022.

doi: 10.21037/jgo-22-619

View this article at: <https://dx.doi.org/10.21037/jgo-22-619>

Introduction

Hepatocellular carcinoma (HCC) is the most common primary liver malignancy and the world's fourth leading cause of cancer-related mortality (1). Liver transplantation and hepatectomy are curative treatments for HCC, and the indications have been safely expanded (2,3). However, some tumors are still too advanced to be cured by surgical resection and orthotopic liver transplantation at diagnosis. Therefore, it is important to administer palliative treatments to achieve downstaging for surgical therapy or delay the progression of tumors. Combination therapy improves the prognosis outcomes of patients with advanced HCC better than single-agent therapy (4), implying that combined therapy could be a promising treatment option for some HCC patients.

In the past few decades, cancer immunotherapy has become one of the most effective treatments and has been validated in various tumors (5,6). Since the advent of immune checkpoint inhibitors (ICIs), the concept of normalizing the tumor immune microenvironment (TIME) by correcting dysfunctions of the immune response has drawn attention again to immunotherapy. Immune checkpoint therapy, which is at the forefront of immunotherapy, has demonstrated clinical activity in several malignancies, including HCC, although the response rate to ICIs varies in patients (7,8). The encouraging results from clinical trials of immune checkpoint therapy have resulted in increased clinical implementation in various types of cancer, including HCC. However, only approximately 20% of advanced HCC patients benefit from ICIs, and most of them have disease progression after 3–9 months (9). These results indicate that a substantial proportion of patients treated with ICIs suffer primary or acquired resistance. Therefore, studying the underlying mechanism and maximizing the curative effect of immune checkpoint therapy has become a focus in the field of HCC treatment.

Members of the tripartite motif (TRIM) protein family are engaged in a wide range of cellular functions and share several functional characteristics (10). The *TRIM* family, consisting of roughly 80 members, is structurally a highly conserved gene family whose family members all contain the RING finger domain, a basic composition of

1 or 2 zinc-finger domains called B boxes, and a coiled-coil region (11). Diverse C-terminal domains determine the primary structural distinctions within the *TRIM* family, and *TRIM* proteins are divided into 11 classes based on their C-terminus (from C-I to C-XI) (12). To date, *TRIM* proteins have been shown to regulate cell proliferation (13,14), facilitate or prevent cancer cell transformation (15), and directly interact with innate immunity (11), among many other roles. It has been shown that multiple *TRIM* genes play a significant function in liver cancer development as well as its immunotherapy (16,17). However, the relationship between *TRIM* genes and the effect of treatment as well as prognosis in HCC is not clear.

Although single *TRIM* family gene has been investigated in various solid tumors, no systematical and comprehensive analysis has been performed to identify the role of *TRIMs* in HCC. Our study aimed to systematically assess *TRIM* family correlations with prognosis, checkpoints, and TIME in HCC. The relationships between clustering subgroups, risk models, checkpoints, immune scores, and immune cell infiltration, and the responsiveness of sorafenib and transarterial chemoembolization (TACE) treatment were subsequently thoroughly analyzed based on *TRIM* family gene-related signatures to further investigate *TRIM* genes' effect on TIME. The development of risk models for *TRIM* genes is vital for helping to improve risk stratification and clinical decision-making in HCC. We present the following article in accordance with the TRIPOD reporting checklist (available at <https://jgo.amegroups.com/article/view/10.21037/jgo-22-619/rc>).

Methods

Datasets

The International Cancer Genome Consortium (ICGC) and The Cancer Genome Atlas (TCGA) databases (<https://daco.icgc.org/> and <https://portal.gdc.cancer.gov/>) were used to obtain RNA sequencing (RNA-seq) transcriptome data and clinical data of HCC patients. The inclusion criteria were: (I) histologically confirmed HCC, and (II) data on mRNA expression profiles and overall survival (OS) available at the same time. Ultimately, 231 samples

Table 1 Clinicopathological features of patients in TCGA and ICGC cohorts

Variables	Datasets, n (%)	
	TCGA	ICGC
Age		
<53 years	101 (27.3)	20 (8.7)
≥53 years	269 (72.7)	211 (91.3)
Gender		
Female	121 (32.7)	61 (26.4)
Male	249 (67.3)	170 (73.6)
Grade		
G1	55 (14.9)	–
G2	177 (47.8)	–
G3	121 (32.7)	–
G4	12 (3.2)	–
Stage		
Stage 1	171 (46.2)	36 (15.6)
Stage 2	85 (23.0)	105 (45.5)
Stage 3	85 (23.0)	71 (30.7)
Stage 4	5 (1.4)	19 (8.2)
M		
M0	266 (71.9)	–
M1	4 (1.1)	–
T		
1	181 (48.9)	–
2	93 (25.1)	–
3	80 (21.6)	–
4	13 (3.5)	–

TCGA, The Cancer Genome Atlas; ICGC, International Cancer Genome Consortium.

of HCC were acquired, together with clinicopathological characteristics such as age, sex, grade, and TNM stage. A total of 231 ICGC HCC patients were assigned to the training cohort, while 370 TCGA patients were assigned to the validation cohort. The baseline clinicopathological features are shown in *Table 1*. The GSE109211 and GSE104580 datasets from the Gene Expression Omnibus (GEO; <https://www.ncbi.nlm.nih.gov/geo/>) database were used to analyze the responsiveness of sorafenib, TACE, and

ICI treatment. The study was conducted in accordance with the Declaration of Helsinki (as revised in 2013).

TRIM genes selection

Based on previously published literature, 62 *TRIM* genes were selected (11). On the basis of mRNA expression results of liver hepatocellular carcinoma (LIHC) from ICGC, a total of 62 *TRIM* genes were identified. Next, the differential expression of 62 *TRIM* genes in tumor tissues and adjacent normal tissues was analyzed.

Bioinformatics analysis

We used the “ConsensusClusterPlus” program to classify HCC patients into different subtypes in order to explore the biological functions of *TRIM* genes in HCC. To examine gene expression patterns among different HCC subtypes, principal component analysis (PCA) was performed using R (v4.1.0). Pathways analysis for different HCC subtypes was carried out using the R software package “GSVA”.

The immune score for each patient was estimated using the R “estimate package” and an algorithm (18). Cell-type identification by calculating relative subsets of RNA transcripts (CIBERSORT; <https://cibersort.stanford.edu/>) was used to develop the fraction of 22 immune cell types for each tumor specimen. With 1,000 permutations, the samples were chosen based on $P < 0.05$.

In the ICGC training cohort, we performed K-M survival analysis for all *TRIM* genes, and we used least absolute shrinkage and selection operator (LASSO) regression analysis to identify predictive risk signatures for above *TRIM* genes ($P < 0.05$). Ten cross-validations were used to select suitable values for the penalty parameter. The LASSO regression approach yielded the coefficients, and the risk score was obtained using the following formula: $\text{Riskscore} = \sum_{i=1}^n \text{coef}_i * x_i$ where coef_i is the coefficient and x_i is the transformed relative expression value of each selected *TRIM* genes. This formula was used to generate a risk score for each patient in the training and validation cohorts. The samples were then separated into high-risk and low-risk categories based on the cutoff (median value).

Data from GEO and Array Express were collected by Tumor Immune Single-cell Hub (TISCH) to formulate a single-cell RNA-seq (scRNA-seq) atlas. TISCH compares different patients, therapy and response groups, tissue origins, cell types, and even cancer types by visualizing gene expression across several data sets at the single-cell or

cluster level. In this study, we employed TISCH datasets to unravel the TME heterogeneity of 8 *TRIM* genes at the single-cell level.

The role of copy number alternations (CNAs) of the *TRIM* family on immune cell infiltration levels was evaluated by applying the Tumor Immune Estimation Resource (TIMER, <https://cistrome.shinyapps.io/timer/>).

Statistical analysis

R version 4.1.0 and GraphPad Prism 9.2 were used for statistical analysis. A Student's *t*-test, chi-square test, and Mann-Whitney-Wilcoxon test were used for comparisons between 2 groups, and a one-way analysis of variance (ANOVA) test was utilized for analysis with multiple comparisons. Survival curves were generated and compared using the Kaplan-Meier method. Univariate and multivariate analyses were conducted with Cox proportional hazards regression models. Receiver operating characteristic (ROC) curves were employed to compare the predictive accuracy of the *TRIM* gene-relevant signatures. $P < 0.05$ (two-sided) indicated statistical significance.

Results

Expression of *TRIM* genes in HCC

Based on the ICGC dataset, we systematically investigated the expression patterns of 62 *TRIM* genes between HCC ($n=240$) and normal tissues ($n=197$) to assess the biological function of *TRIM* genes in the initiation and development of HCC. The expression levels of *TRIM* genes in HCC and normal tissues were evident (Figure S1A,S1B). The expression levels of most *TRIM* genes (45 of 62) were higher in HCC tissues than in normal adjacent tissues. Some *TRIM* genes (7 of 62) were lower in HCC tissues than in normal tissues (Figure S1A,S1B, Table S1). Additionally, there were also *TRIM* genes (10 of 62) with no statistically significant difference ($P > 0.05$). The above results revealed that *TRIM* genes might possess essential biological roles in HCC development.

Significant correlation of consensus clustering for *TRIM* genes with the characteristics and survival of HCC patients

To achieve optimum clustering stability, $k=2$ was determined, and the samples from 231 patients with HCC were divided into 2 subgroups (Figure 1A). Individual *TRIM*

gene expression was lower in cluster 1 than it was in cluster 2 (Figure 1B). Next, the clinicopathological characteristics of the 2 subgroups were compared (Figure 1B). Cluster 2 was more significantly related to higher stage ($P < 0.01$) and higher mortality than cluster 1. Cluster 1 had a superior OS ($P < 0.001$; Figure 1C). The results of PCA found that the gene expression profiles of the 2 groups were well differentiated (Figure 1D).

Association of immune check points with *TRIM* family

We looked at differential expression in 2 subtypes and the relationship between immune checkpoints and *TRIM* genes to see whether immune checkpoints were related. The expression level of *KIR2DL1*, *KIR2DL3*, *KIR2DL2*, *KLRC1*, *LAG3*, *CD274*, *CTLA4*, and *TIGIT* were downregulated in HCC tissues compared with normal tissues ($P < 0.05$; Figure 2A). *CTLA4*, *HAVCR2*, and *PDCD1* expression levels in cluster 2 were significantly higher than in cluster 1 ($P < 0.05$; Figure 2B). *NT5E* expression, on the other hand, was lower in cluster 2 than in cluster 1 ($P < 0.05$; Figure 2B). We then analyzed the correlation between *TRIM* genes and the immune checkpoints (*PDCD1*, *NT5E*, *HAVCR2*, and *CTLA4*) in ICGC and TCGA datasets, which showed that a number of *TRIM* genes had a significant correlation with immune checkpoints, as shown in Figure 2C,2D. The above results suggested that *TRIM* family genes may improve immunotherapy for HCC.

Consensus clustering for *TRIM* genes associated with distinct immune cell infiltration

To investigate the effect of *TRIM* genes on the TIME of HCC, we compared the immune infiltrate levels in cluster 1 and cluster 2 (Figure 2E). This analysis showed a significant difference in naive B cells, memory B cells, regulatory T cells (Tregs), gamma delta T cells, M0 macrophages, M1 macrophages, resting dendritic cells, and stromal score between the 2 clusters (Figure 2E). Cluster 1, with a higher stromal score, had a better prognosis than cluster 2, with a lower stromal score ($P < 0.05$). We further performed gene set variation analysis (GSVA) and the results showed that the spliceosome, homologous recombination, and DNA replication pathway might be implicated in the distinct TIME of cluster 2 ($P < 0.0001$; Figure 3A), while amino acid metabolism, fatty acid metabolism, and the drug metabolism cytochrome P450 pathway might be implicated in the distinct TIME of cluster 1 ($P < 0.0001$; Figure 3A, Table S2).

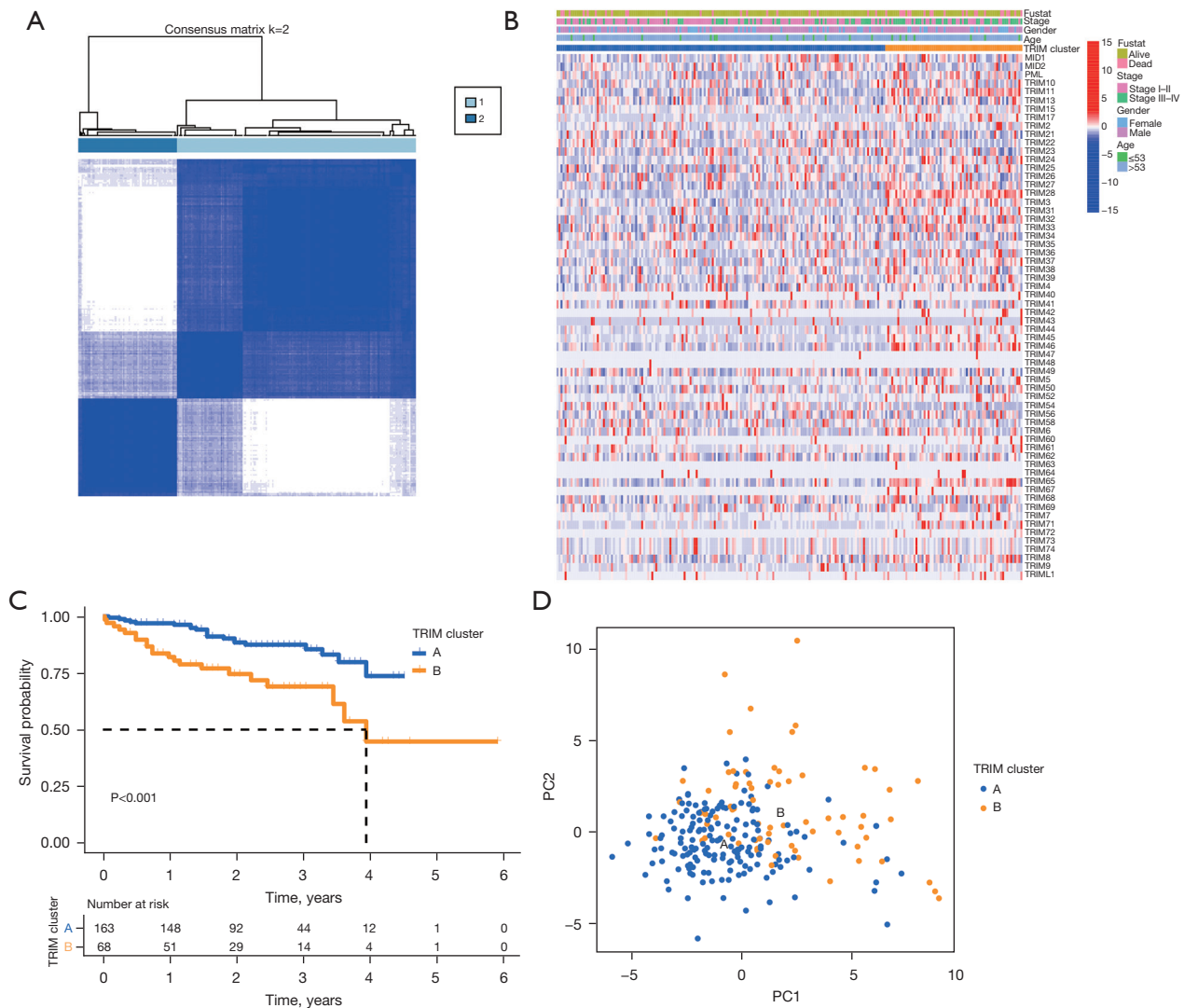


Figure 1 Differential clinicopathological features and survival of HCC in cluster 1/2 subtypes in ICGC cohort. (A) Consensus clustering matrix for $k=2$. (B) Heatmap and clinicopathologic features of the 2 clusters (cluster 1/2). (C) Kaplan-Meier curves of OS for patients with HCC in 2 clusters (cluster 1/2). (D) Principal component analysis of the total mRNA expression profile in 231 patients with HCC. HCC, hepatocellular carcinoma; ICGC, International Cancer Genome Consortium; OS, overall survival; TRIM, tripartite-motif; PC, principal component.

Hence, the metabolism-related signaling pathways might be implicated in the distinct TIME of cluster 1.

Construction and validation of prognostic signatures for TRIM genes

A total of 231 ICGC HCC patients were assigned to the training group, while 370 TCGA patients were assigned to the validation cohort (Table 1). We conducted univariate analysis for TRIM genes, and the results showed that 12

TRIM genes (*MID1*, *TRIM11*, *TRIM21*, *TRIM22*, *TRIM24*, *TRIM28*, *TRIM31*, *TRIM37*, *TRIM42*, *TRIM47*, *TRIM5*, are *TRIM74*) were related to survival in HCC (all $P < 0.05$; Figure 3B, Table S3).

To accurately predict the clinical prognosis of HCC patients, we performed K-M survival analysis for all TRIM genes, and we used least absolute shrinkage and selection operator (LASSO) regression analysis to identify predictive risk signatures for above TRIM genes ($P < 0.05$). The results showed that 9 TRIM genes, namely *MID1*, *TRIM38*,

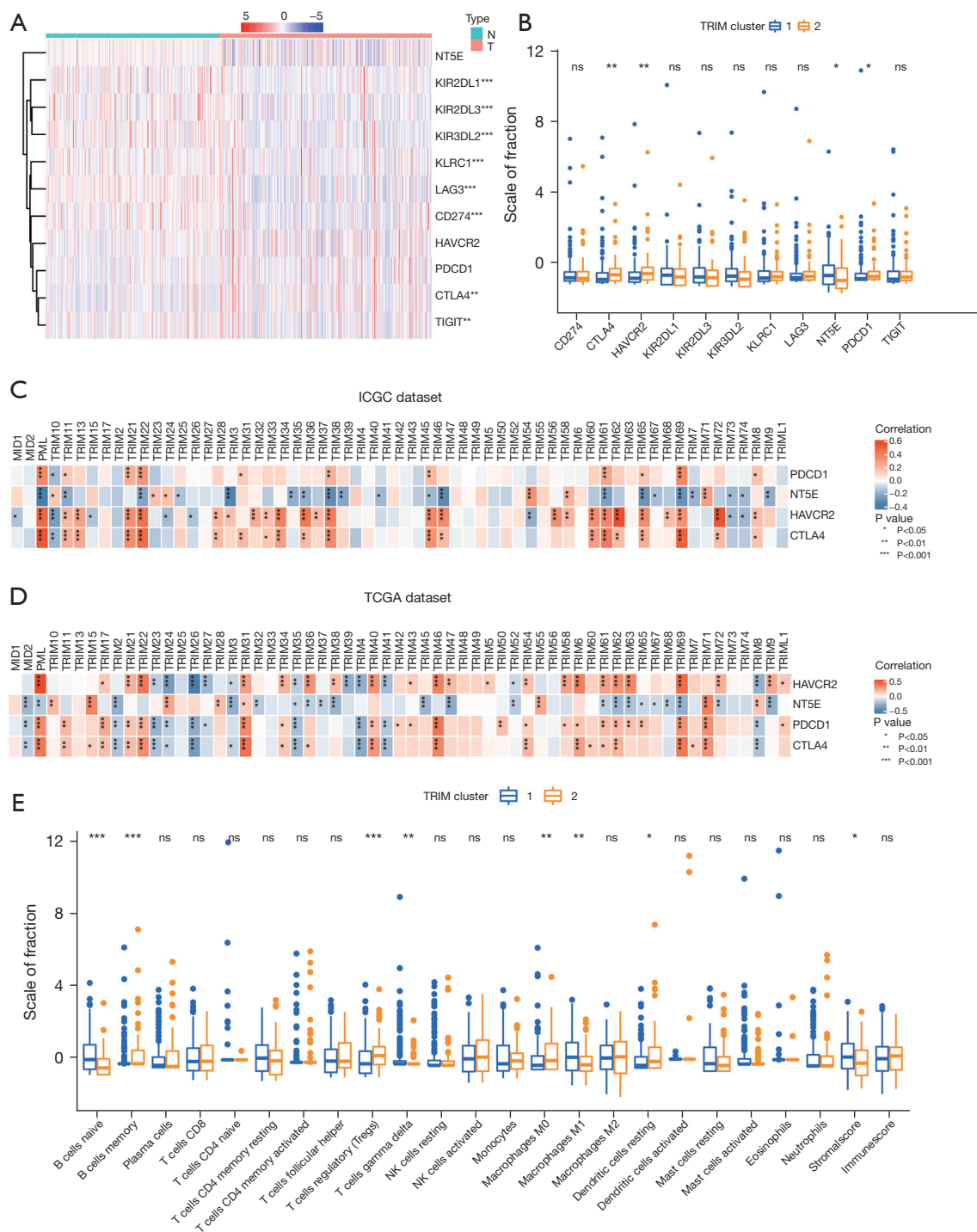


Figure 2 Association of immune check points with *TRIM* genes and the landscape of immune cell infiltration in HCC. (A) Tumor *vs.* normal; (B) cluster 1 *vs.* cluster 2; (C) ICGC dataset; (D) TCGA dataset; (E) landscape of immune cell infiltration in cluster 1/2. * $P < 0.05$, ** $P < 0.01$, and *** $P < 0.001$. TRIM, tripartite-motif; HCC, hepatocellular carcinoma; ICGC, International Cancer Genome Consortium; TCGA, The Cancer Genome Atlas; ns, no significance.

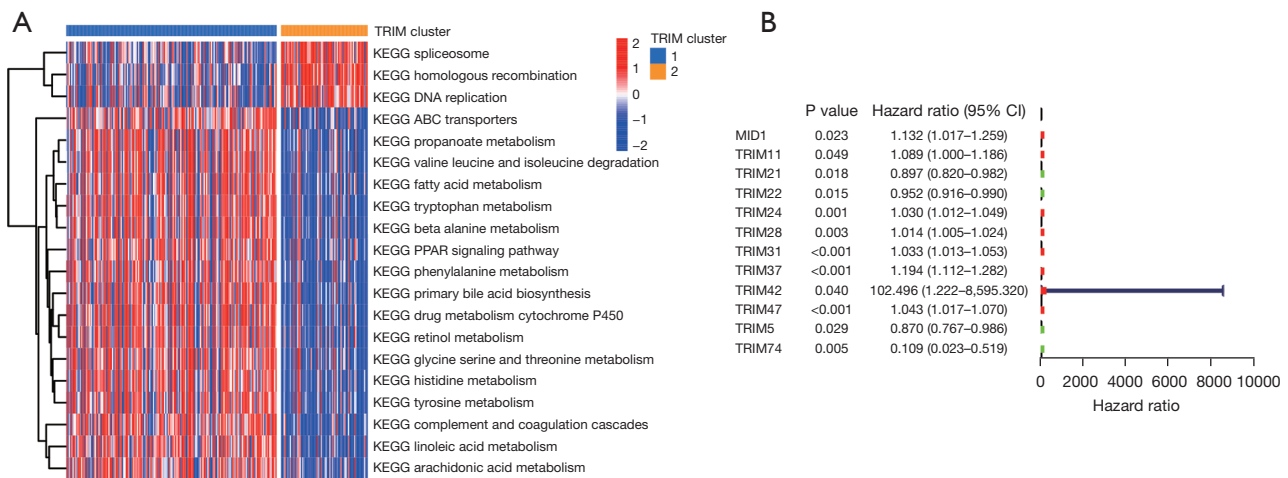


Figure 3 The potential regulatory mechanisms resulting in differences in TIME. (A) The potential regulatory mechanisms resulting in differences in TIME between the 2 subgroups by performing GSVA; (B) univariate analyses in the ICGC training cohort. TIME, tumor immune microenvironment; GSVA, gene set variation analysis; ICGC, International Cancer Genome Consortium.

TRIM37, *TRIM47*, *TRIM24*, *TRIM28*, *TRIM22*, *TRIM5*, and *TRIM74*, were identified. The median risk score (median =0.5656) was then used to separate patients into low- and high-risk groups (Table S4). The distribution of risk scores, OS, OS status, and expression profiles of the 9 *TRIM* gene-based signatures in the ICGC training and TCGA validation cohorts are shown in Figure 4. The heatmap data showed that *TRIM* genes, including *MID1*, *TRIM28*, *TRIM31*, *TRIM37*, and *TRIM47*, were substantially expressed in the high-risk group (Figure 4). In the ICGC training and TCGA validation cohorts, the low-risk group had a longer OS than the high-risk group ($P<0.05$; Figure 4). We then performed univariate and multivariate analyses and found that risk score was an independent prognostic factor in the ICGC and TCGA datasets (all $P<0.05$; Figure 5). We compared the respective area under curve (AUC) values in 1-, 3-, and 5-year ROC curve analyses to determine the prognostic accuracy of our model. The 1-, 3-, and 5-year AUC values for the 9 risk signatures in the ICGC training cohort were 0.789, 0.827, and 0.694, respectively (Figure 5), and 0.642, 0.571, and 0.533 in the TCGA dataset, respectively (Figure 5). Our model, based on the 9 *TRIM* genes, demonstrated favorable discrimination performance for the prognosis of patients with HCC, as evidenced by the AUC values. The results of PCA analysis corroborated the preceding findings (Figure S2). These findings suggested that the risk score derived from the 9 risk signatures might reliably predict HCC patients' prognosis.

Risk scores correlated with stage, immune score, TRIM cluster, and therapies in HCC

The association between risk score and clustering subtypes, stage, immune score, estimate score, stromal score, tumor purity, and OS status was also investigated. The cluster 2 risk score was significantly greater than the cluster 1 risk score ($P<0.001$; Figure 6). The high-risk group had a significantly lower immune score and higher TNM stage than the low-risk group ($P<0.01$; Figure 6).

The heatmap depicted the expression levels of 9 *TRIM* genes in the ICGC training cohort's high- and low-risk groups (Figure 6). The high-risk group had lower levels of *TRIM38*, *TRIM22*, *TRIM5*, and *TRIM74* expression than the low-risk group. *TRIM31*, *TRIM47*, *TRIM28*, *TRIM37*, and *MID1* expression levels were low in the low-risk group. In addition, we analyzed the correlation of the 9 prognostic *TRIM* genes with TNM stage in the ICGC and TCGA datasets, and the result showed that in the ICGC dataset, there was a clear positive correlation between the expression of *TRIM28* and *TRIM47* and TNM stage, and similar results could be obtained in the TCGA dataset (Figure S3).

Immunotherapy, TACE, and molecularly targeted therapies have been widely used in the treatment of patients with HCC and contribute to the prognosis of patients. We investigated whether *TRIM* genes harbored the same influence on ICIs, sorafenib, and TACE treatment in additional HCC cases. First, we employed the tumor immune dysfunction and exclusion (TIDE)

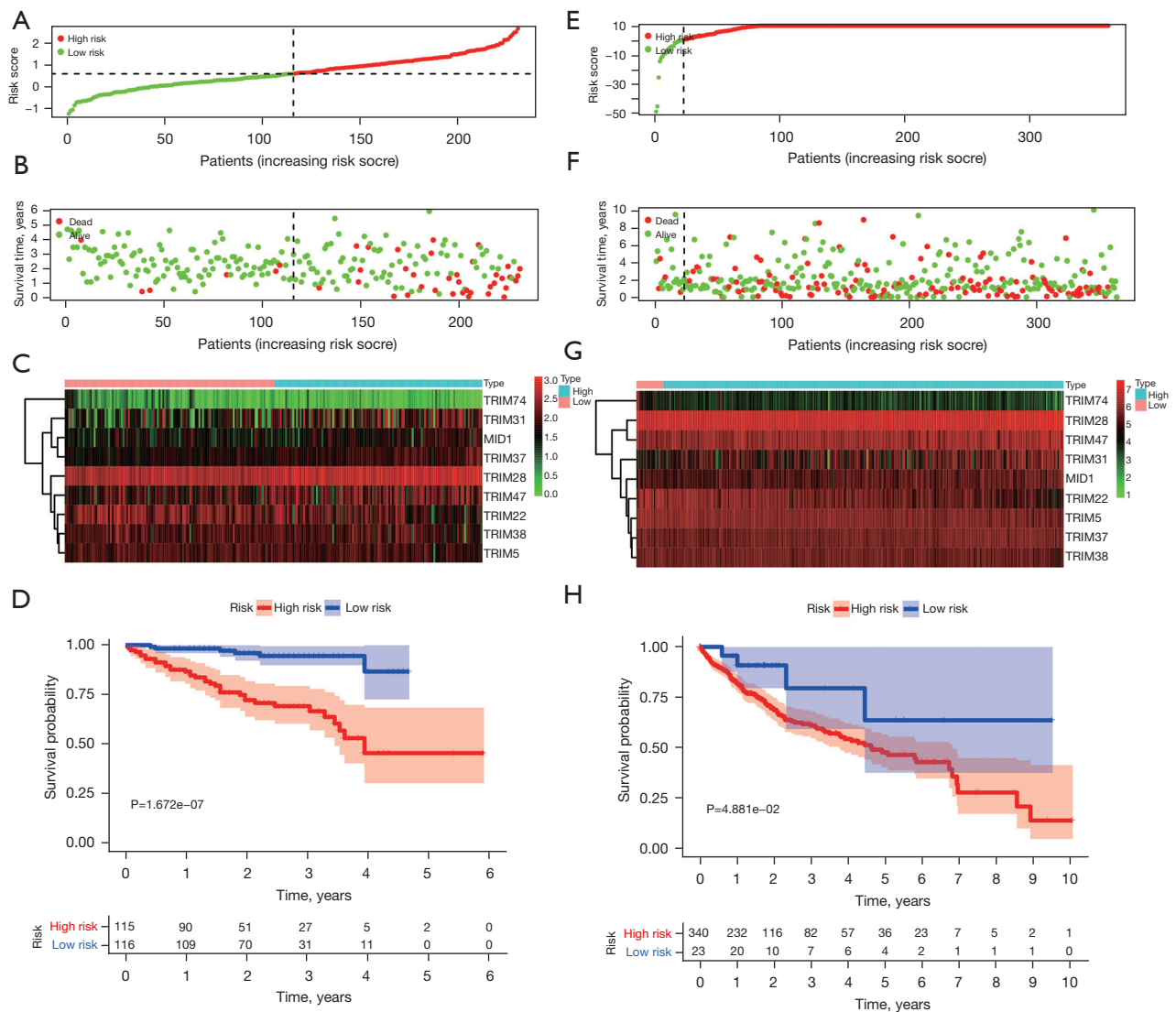


Figure 4 Construction and validation of prognostic signatures of *TRIM* genes in ICGC and TCGA cohorts. (A-D) Distribution of risk score, OS, and OS status and heatmap of the 9 prognostic *TRIM* genes in the ICGC training cohort; (E-H) distribution of risk score, OS, and OS status and heatmap of the 9 prognostic *TRIM* genes in the TCGA validation cohort. TRIM, tripartite-motif; ICGC, International Cancer Genome Consortium; TCGA, The Cancer Genome Atlas; OS, overall survival.

score, a scoring system that integrates 2 tumor immune escape mechanisms, to analyze the response rate of HCC immunotherapy. A high TIDE score indicates a poor treatment effect for ICIs (19). The results showed that the TIDE score of high-risk patients was high, but the response rate of immunotherapy in low-risk patients was higher than that in high-risk patients (87% vs. 65%; Figure 7A, 7B). Next, we selected the eligible GEO datasets, GSE109211 and GSE104580, as the external validation cohort. The response to sorafenib was not

significantly different from the risk score, but the response rate was significantly higher in low-risk patients than in high-risk patients (42% vs. 24%; Figure S4A, Figure 7C, Table S5), which was possibly due to the small number of patients who responded to sorafenib. In addition, the response to TACE was significantly different from the risk score, and the response rate was higher in low-risk patients than in high-risk patients (65% vs. 39%; Figure S4B, Figure 7D, Table S6).

Single-nucleotide variant (SNV) mutations are associated

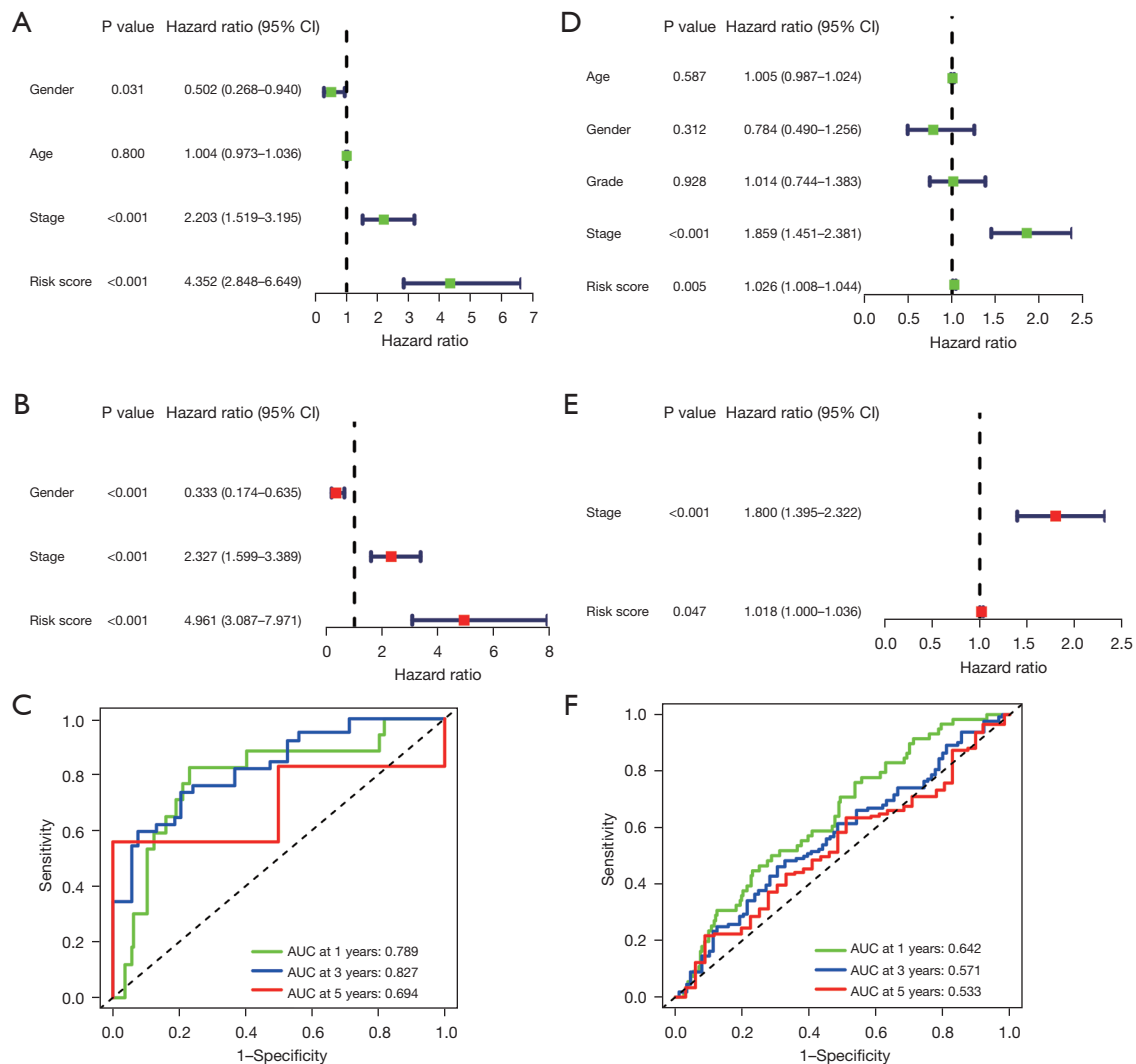


Figure 5 Univariate, multivariate Cox regression and ROC analyses in the 2 cohorts. Univariate (A) and multivariate (B) Cox regression analyses in the ICGC training cohort; univariate (D) and multivariate (E) Cox regression analyses in the TCGA validation cohort; receiver operating characteristic curves of 1, 3, and 5 years based on the risk score in the ICGC training cohort (C) and TCGA validation cohort (F). ICGC, International Cancer Genome Consortium; TCGA, The Cancer Genome Atlas.

with HCC treatment efficacy prediction and immune infiltration (20), so specific mutations in high- and low-risk groups may bring benefits for the prognosis of patients. We compared HCC samples from the low *TRIM* score subgroup to those from the high *TRIM* score subgroup in terms of substantially modified genes (*SMG*). The *SMG* mutational landscapes revealed that in the high *TRIM* score group, TP53 (17% vs. 47%) had greater somatic mutation rates, whereas in the low *TRIM* score group, CTNNB1 (34% vs. 23%) had higher somatic mutation rates (Figure S5A,S5B).

Correlation between *TRIM* genes and the TISH database

We used TISCH to investigate the expression of the *TRIM* genes in the HCC tumor microenvironment at the single-cell level (Figure 8A–8I). In LIHC_GSE140228, most *TRIM* genes were mainly expressed in immune cells, including B cells, plasma cells, exhausted CD8T (Tex) cells, CD8T cells, CD4 conventional T (Tconv) cells, mono/macrophages, mast cells, Tpolif cells, natural killer (NK) cells, and regulatory T cells. These results suggested that the expression of *TRIM* genes in HCC was closely related

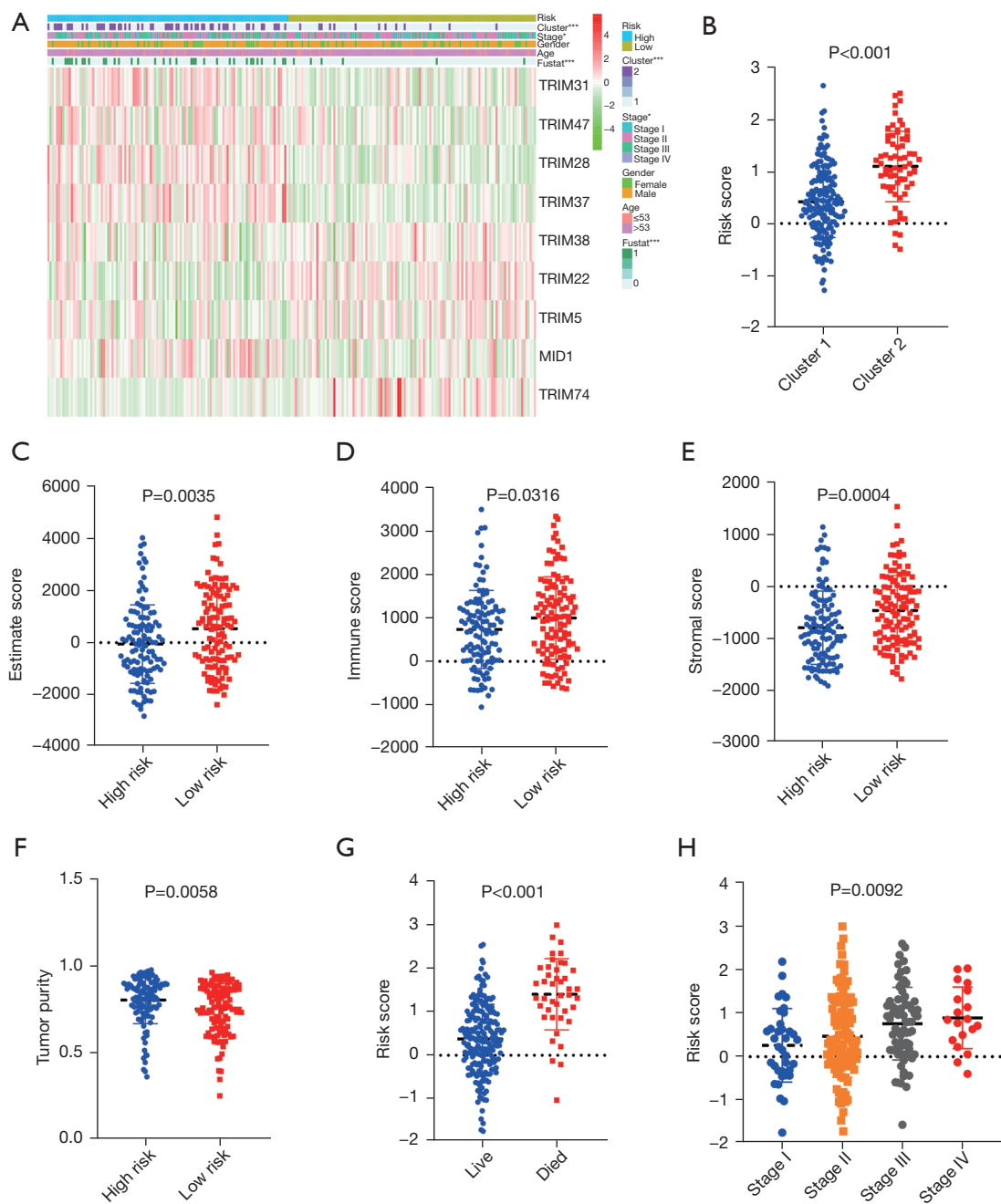


Figure 6 Prognostic risk scores correlated with clinicopathological features, estimate score, stromal score, tumor purity, OS status, TNM stage, and immune score in TCGA training cohort. (A) Heatmap and clinicopathological features of high- and low-risk groups. (B-H) Distribution of risk scores stratified by cluster 1/2 (B), estimate score (C), immune score (D), stromal score (E), tumor purity (F), OS status (G), and TNM stage (H). * $P < 0.05$, and *** $P < 0.001$. OS, overall survival; TCGA, The Cancer Genome Atlas.

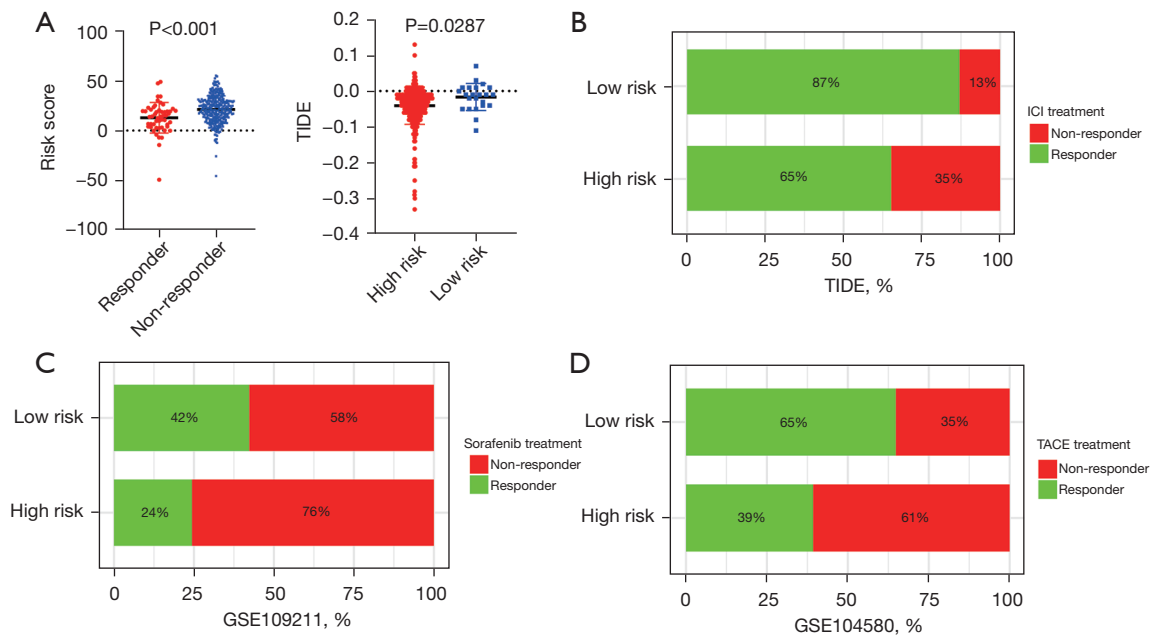


Figure 7 Prognostic risk scores correlated with TIDE score, sorafenib and TACE treatment. (A) Prognostic risk scores correlated with TIDE score; (B) the response to ICI treatment; the response to sorafenib treatment (C) and TACE treatment (D). TIDE, tumor cell dysfunction and exclusion; ICIs, immune checkpoint inhibitors; TACE, transarterial chemotherapy embolization.

to immune cell infiltration (Figure 8).

Effect of genetic alterations of the TRIM gene signatures on immune cell infiltration

We used TIMER 2.0 to analyze the relationship of 9 TRIM genes with infiltration levels of 6 immune cell types to assess the effect of the 9 TRIM genes on the HCC immune microenvironment. The results revealed that a significantly positive correlation was observed between almost all the immune cells and the 9 TRIM genes (Figures S6,S7). These results confirmed that TRIM gene-based risk signatures were implicated in the TIME of HCC.

Genome instability and immune cell infiltration are both promoted by somatic CNAs. The infiltration levels of B cells, CD4⁺ T cells, CD8⁺ T cells, neutrophils, macrophages, and dendritic cells in HCC were significantly impacted by the CNAs of the identified TRIM gene signatures, including arm-level deletion and arm-level gain (Figure 9). These findings showed that TRIM genes were important regulators of TIME in HCC patients.

Finally, we performed copy number variation (CNV) analysis on 9 TRIM genes, and the results showed that all 9 genes had acquired mutations greater than deletion

mutations (Figure 10A). In addition, we labeled the location of the 9 TRIM genes on the chromosome, as shown in Figure 10B. Further analysis showed that in MID1, the alteration frequency of deep deletion and amplification accounted for the vast majority, but in TRIM5 and TRIM28, both accounted for half. In addition, the alteration frequency of amplification occupied almost all of the other TRIM genes (Figure 10C). The results of the abovementioned studies indicated that the genomic and transcriptomic landscapes had significant differences and connections.

Discussion

The expression patterns, prognostic values, and effects on TIME of the TRIM genes in HCC were investigated in this study. In HCC tissues, the expression of 45 TRIM genes increased significantly, while the expression of 7 TRIM genes dropped dramatically. By using consensus clustering for TRIM genes, we were successful in identifying subgroups of HCC: cluster 1 and cluster 2. The cluster subtype affected the prognosis and different clinicopathological features of HCC and was closely related to immune cell infiltration levels. We characterized the effects of differential TRIM genes on different HCC subtypes by clustering TRIM

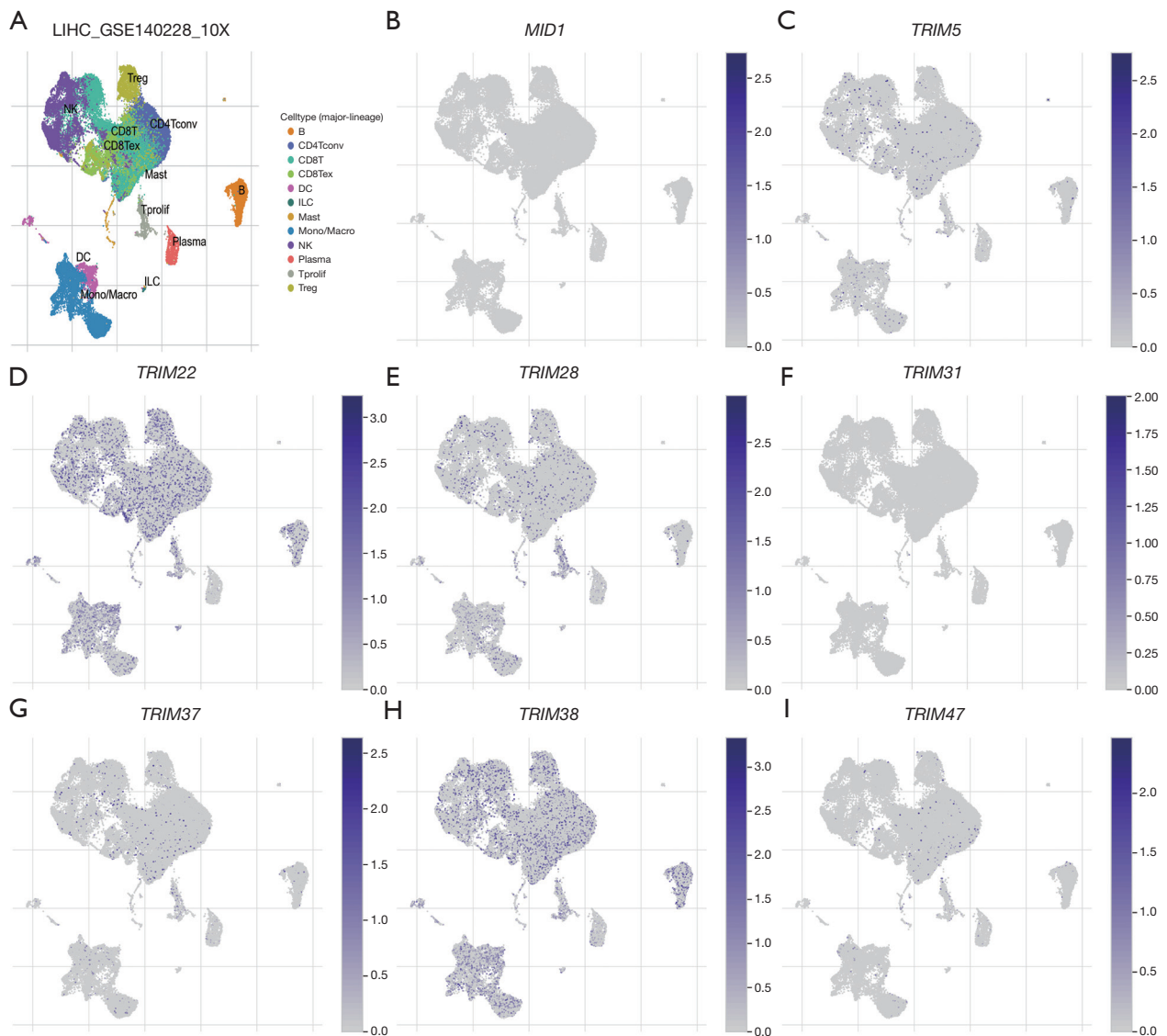


Figure 8 The cell types and their distribution in the LIHC_GSE140228 datasets. (A) The distribution of 8 *TRIM* genes in different cell types was analyzed using single-cell resolution in the LIHC_GSE140228 datasets. *MID1* (B), *TRIM5* (C), *TRIM22* (D), *TRIM28* (E), *TRIM31* (F), *TRIM37* (G), *TRIM38* (H), and *TRIM47* (I). LIHC, liver hepatocellular carcinoma; *TRIM*, tripartite-motif.

genes. The patients in cluster 1 showed a lower TNM stage. Similarly, cluster 1 had a better survival rate compared with that of cluster 2.

Furthermore, we analyzed and summarized the prognostic predictive role of *TRIM* family genes in HCC, and finally derived 9 prognostic risk signatures from *TRIM* genes, which effectively stratified the OS of HCC patients in the ICGC and TCGA cohorts into high- and low-risk groups. The risk score was found to be an independent prognostic factor for HCC patients in both univariate and multivariate

cox regression models. The high- and low-risk groups were also related to distinct clustering subtypes, TNM stage, immune score, estimate score, tumor purity, and stromal score. Among these risk signatures, *MID1*, known as *TRIM18*, functions as an oncogene in melanoma (21). *TRIM31*, *TRIM28*, *TRIM37*, and *TRIM47* are involved in oncogenic regulation in HCC, gastric cancer, prostate cancer, and renal cell carcinoma, respectively (22–25). Interestingly, *TRIM37* has emerged as a tumor-suppressive regulator in various tumors in *TRIM37* knock-out mice.

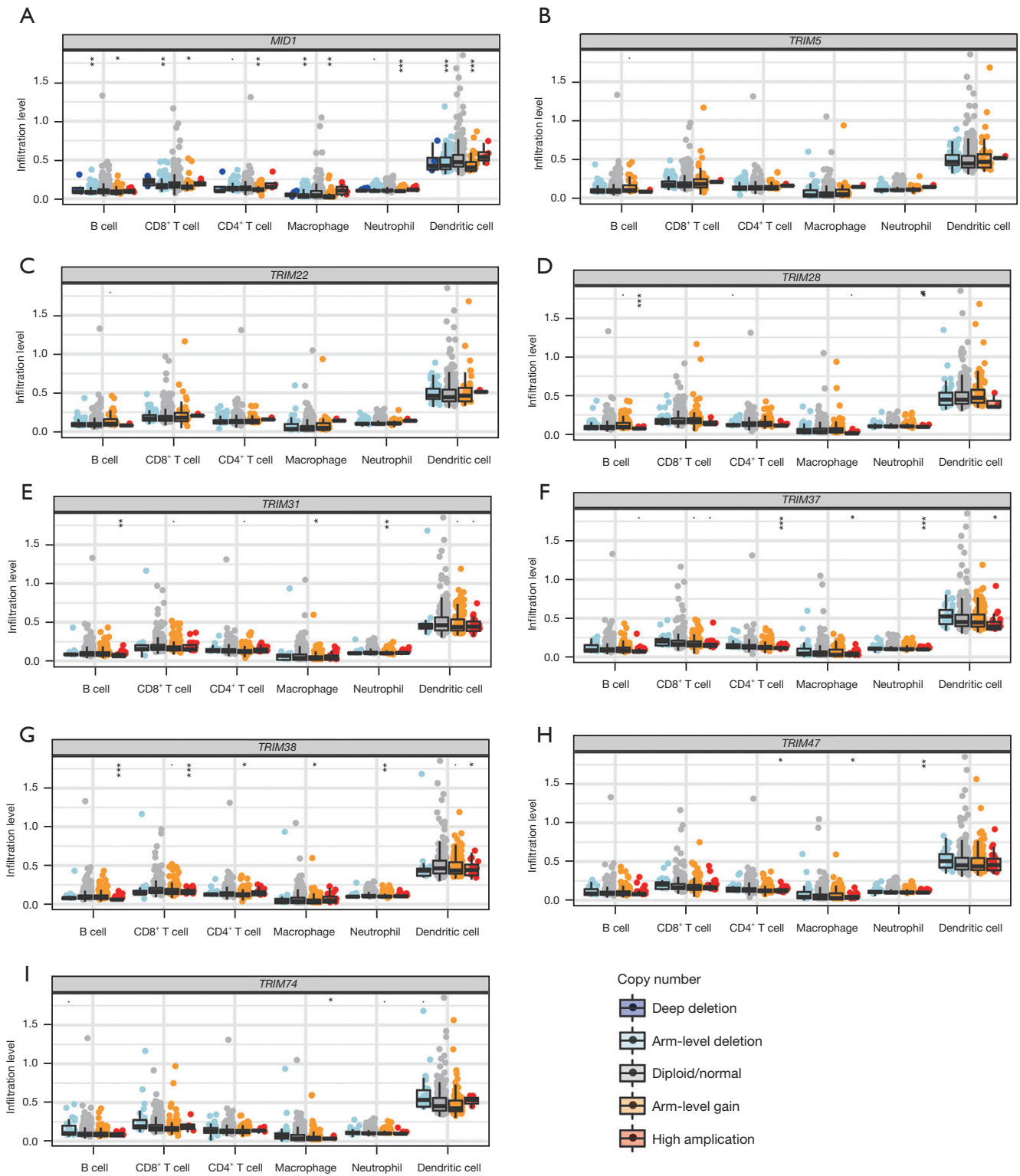


Figure 9 Effect of genetic alterations of *TRIM* gene-relevant signature on the immune cell infiltration. (A-I) *MID1* (A), *TRIM5* (B), *TRIM22* (C), *TRIM28* (D), *TRIM31* (E), *TRIM37* (F), *TRIM38* (G), *TRIM47* (H), and *TRIM74* (I). *P<0.05, **P<0.01, and ***P<0.001. *TRIM*, tripartite-motif.

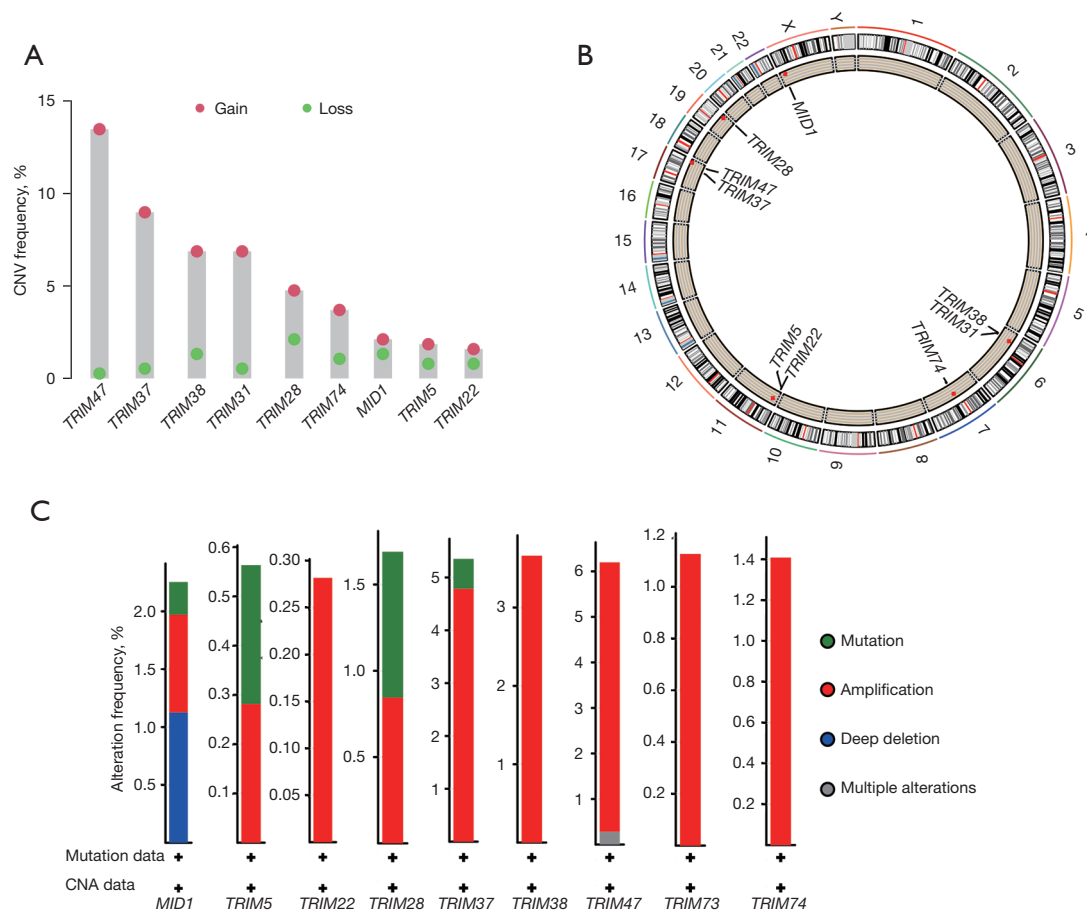


Figure 10 CNV frequency, location and alteration frequency of prognostic *TRIM* genes. CNV frequency of 9 prognostic *TRIM* genes (A). Location of *TRIM* genes on chromosomes (B). Alteration frequency of 9 prognostic *TRIM* genes (C). CNV, copy number variation; *TRIM*, tripartite-motif.

TRIM22 is a double-edged sword in that it is a tumor-suppressive regulator in endometrial cancer and gastric cancer (26,27) but is involved in oncogenic regulation in non-small cell lung cancer and chronic myeloid leukemia (28,29). There are few studies of *TRIM38* and *TRIM74* in tumors, and currently, research mainly focuses on innate immunity and inflammatory response (30,31). These findings demonstrated that deregulation of specific *TRIM* genes played separate functions in various cancers.

To further interrogate the mechanism of the role of *TRIM* family genes in HCC, we performed GSVA analysis and the results indicated that the malignant functional features of the tumor, including amino acid metabolism, fatty acid metabolism, and the drug metabolism cytochrome P450 pathway, were significantly enriched in cluster 1. This may be related to the high response of cluster 1 to sorafenib, TACE, as well as immunotherapy, which in turn

had a better prognosis than cluster 2. Previous research has shown that *RIPK3*-dependent *TRIM28* inhibition in cancer cells leads to increased immunostimulatory cytokine production in the tumor microenvironment, which contributes to strong cytotoxic antitumor immunity (32). Liu *et al.* discovered that *TRIM28* knockdown increases sensitivity to etoposide by upregulating *E2F1* in non-small cell lung cancer (33). Previous study indicated that the expression level of *TRIM37* significantly increased in 354 HCC tissues and promoted peroxisomal matrix protein import via direct monoubiquitination of *PEX5* at K464 and silencing of gene expression through monoubiquitination of histone *H2A* (34). Clinical data analysis has suggested that patients with high expression of *TRIM37* have more sorafenib resistance and shorter disease-free survival (DFS) and OS ($P < 0.01$) (34). In addition, previous research reported that *TRIM47* overexpression played a

role in colorectal cancer chemoresistance in response to fluorouracil (5-FU) therapy (35). To date, *TRIM38* and *TRIM74* have been poorly studied in tumors, and their role in tumors may require more attention and investigation in the future. The above results were consistent with our study results; that is, patients in the high-risk group had a low response to both sorafenib treatment and TACE treatment, and had a poor prognosis. This suggested that for high-risk patients, new treatment strategies may need to be developed to improve survival rates. The predictive significance of the *TRIM* gene-relevant signatures was assessed in HCC patients and validated in the TCGA cohort, as well as the external GSE109211 and GSE104580 cohorts. The results showed that the *TRIM* gene-associated risk profiles could effectively predict the prognosis of HCC patients, allowing for more personalized treatment options and greater insight into the advancement of therapeutic techniques.

Previous studies have shown a close relationship between gene mutations and tumor development prognosis as well as treatment (36-38). Simultaneously, numerous research findings have revealed that the most common mutant gene mutations in HCC are, among others, *TP53* and *CTNNB1*, which are closely connected to the prognosis and therapies of HCC (36-38). At the same time, we also found that the most frequent type of non-nonsense mutation, whether in the low- or high-risk group, was a missense mutation. The top 3 genes with the highest frequency were *TP53*, *TTN*, and *CTNNB1*, respectively, which was consistent with previous studies (39,40). However, we found that the genes with the highest mutation frequency among high- and low-risk groups differed, with *CTNNB1* highest in the low-risk group and *TP53* highest in the high-risk group. Therefore, we may be able to distinguish whether a patient belongs to a high- or low-risk group by the specific gene mutated.

Although there are many models related to the prognosis and treatment of HCC, in this study, the risk prognostic model could distinguish well high and low risks by prognosis-related *TRIM* genes. In addition, the model could also distinguish well the response of HCC patients to immunotherapy, targeted therapy, and TACE, providing new insights and theories for precise, personalized treatment of HCC patients. In this study, the risk score based on the 9 *TRIM* gene-based risk signatures was shown to be strongly related to immune cell infiltration. These findings suggested that *TRIM* genes are involved in TIME regulation to some extent. In addition, the advent of ICIs has brought great benefits to cancer patients, and HCC

patients are no exception, but not all patients can benefit from the treatment of ICIs. The immune checkpoint (*CTLA4*, *HAVCR2*, and *PDCD1*) expression levels of cluster 2 were significantly higher than that of cluster 1. The immunotherapy response of HCC is very low (about 10%), and our risk model could distinguish well which patients responded to immunotherapy, which in turn may improve the immunotherapy effect. To evaluate the response of HCC patients to immunotherapy, we employed the TIDE score, with the results showing that the low-risk score group had a low TIDE score but a high response to ICI treatment. Therefore, we proved that the *TRIM* family gene-based prognostic model could evaluate well the degree of benefit of immunotherapy in patients at different risk levels, leading to the implementation of personalized treatment strategies for different patients, ultimately benefiting patients.

Our research did, however, have some limitations. For instance, our findings were confirmed in the ICGC, TCGA, and GEO cohorts, but we didn't have any independent clinical sample data to support our claims and conclusions. Thus, the results of our research will need to be verified further, and we will continue to investigate *TRIM* gene correction and TIME in HCC in the future. In addition, the *TRIM* family's regulatory mechanism in TIME should be explored further in order to restructure TIME and improve HCC precision immunotherapy.

Conclusions

In conclusion, this research examined the prognostic significance, immune checkpoint correlations, TIME relevance, and potential regulatory mechanisms of *TRIM* genes in HCC. The risk score established from 9 *TRIM* gene-based signatures was found to be an independent prognostic indicator for HCC patients. TACE and ICI treatment were more likely to benefit patients with a low-risk score. The levels of immune cell infiltration in patients with HCC were strongly associated with the *TRIM* gene-based signatures. Further, many signaling pathways may be implicated in the regulation of the HCC immune microenvironment by the *TRIM* family. The identification of *TRIM* genes that contribute to biochemical pathways controlling tumor immune responses, as well as examining their regulatory processes and responses, could provide potential targets for enhancing HCC's immunotherapy responsiveness.

Acknowledgments

Funding: This work was funded by the National Natural Science Foundation of China (Nos. 81871909, 81702861), the “13th five-year Plan” Science and Education Strong Health Project Innovation team of Yangzhou (Nos. LJRC20181; YZCXTD201801), Provincial-level discipline leader of the NJPH (No. DTRC201809), and Beijing GanDanXiangZhao Public Welfare Foundation Project (No. GDXZ-08-19).

Footnote

Reporting Checklist: The authors have completed the TRIPOD reporting checklist. Available at <https://jgo.amegroups.com/article/view/10.21037/jgo-22-619/rc>

Conflicts of Interest: All authors have completed the ICMJE uniform disclosure form (available at <https://jgo.amegroups.com/article/view/10.21037/jgo-22-619/coif>). The authors have no conflicts of interest to declare.

Ethical Statement: The authors are accountable for all aspects of the work in ensuring that questions related to the accuracy or integrity of any part of the work are appropriately investigated and resolved. The study was conducted in accordance with the Declaration of Helsinki (as revised in 2013).

Open Access Statement: This is an Open Access article distributed in accordance with the Creative Commons Attribution-NonCommercial-NoDerivs 4.0 International License (CC BY-NC-ND 4.0), which permits the non-commercial replication and distribution of the article with the strict proviso that no changes or edits are made and the original work is properly cited (including links to both the formal publication through the relevant DOI and the license). See: <https://creativecommons.org/licenses/by-nc-nd/4.0/>.

References

- Yang JD, Hainaut P, Gores GJ, et al. A global view of hepatocellular carcinoma: trends, risk, prevention and management. *Nat Rev Gastroenterol Hepatol* 2019;16:589-604.
- Ma KW, Cheung TT. Surgical resection of localized hepatocellular carcinoma: patient selection and special consideration. *J Hepatocell Carcinoma* 2017;4:1-9.
- Xu DW, Wan P, Xia Q. Liver transplantation for hepatocellular carcinoma beyond the Milan criteria: A review. *World J Gastroenterol* 2016;22:3325-34.
- Finn RS, Qin S, Ikeda M, et al. Atezolizumab plus Bevacizumab in Unresectable Hepatocellular Carcinoma. *N Engl J Med* 2020;382:1894-905.
- Sanmamed MF, Chen L. A Paradigm Shift in Cancer Immunotherapy: From Enhancement to Normalization. *Cell* 2018;175:313-26.
- Sprinzl MF, Galle PR. Current progress in immunotherapy of hepatocellular carcinoma. *J Hepatol* 2017;66:482-4.
- Postow MA, Callahan MK, Wolchok JD. Immune Checkpoint Blockade in Cancer Therapy. *J Clin Oncol* 2015;33:1974-82.
- Sharma P, Allison JP. Immune checkpoint targeting in cancer therapy: toward combination strategies with curative potential. *Cell* 2015;161:205-14.
- Harding JJ. Immune checkpoint blockade in advanced hepatocellular carcinoma: an update and critical review of ongoing clinical trials. *Future Oncol* 2018;14:2293-302.
- Short KM, Cox TC. Subclassification of the RBCC/TRIM superfamily reveals a novel motif necessary for microtubule binding. *J Biol Chem* 2006;281:8970-80.
- Hatakeyama S. TRIM Family Proteins: Roles in Autophagy, Immunity, and Carcinogenesis. *Trends Biochem Sci* 2017;42:297-311.
- Carthagena L, Bergamaschi A, Luna JM, et al. Human TRIM gene expression in response to interferons. *PLoS One* 2009;4:e4894.
- Lv D, Li Y, Zhang W, et al. TRIM24 is an oncogenic transcriptional co-activator of STAT3 in glioblastoma. *Nat Commun* 2017;8:1454.
- Czerwińska P, Mazurek S, Wiznerowicz M. The complexity of TRIM28 contribution to cancer. *J Biomed Sci* 2017;24:63.
- Bhatnagar S, Gazin C, Chamberlain L, et al. TRIM37 is a new histone H2A ubiquitin ligase and breast cancer oncoprotein. *Nature* 2014;516:116-20.
- Huang XQ, Zhang XF, Xia JH, et al. Tripartite motif-containing 3 (TRIM3) inhibits tumor growth and metastasis of liver cancer. *Chin J Cancer* 2017;36:77.
- Li L, Dong L, Qu X, et al. Tripartite motif 16 inhibits hepatocellular carcinoma cell migration and invasion. *Int J Oncol* 2016;48:1639-49.
- Yoshihara K, Shahmoradgoli M, Martínez E, et al. Inferring tumour purity and stromal and immune cell admixture from expression data. *Nat Commun* 2013;4:2612.
- Jiang P, Gu S, Pan D, et al. Signatures of T cell

- dysfunction and exclusion predict cancer immunotherapy response. *Nat Med* 2018;24:1550-8.
20. Balmain A. The critical roles of somatic mutations and environmental tumor-promoting agents in cancer risk. *Nat Genet* 2020;52:1139-43.
 21. Xia Y, Zhao J, Yang C. Identification of key genes and pathways for melanoma in the TRIM family. *Cancer Med* 2020;9:8989-9005.
 22. Guo P, Ma X, Zhao W, et al. TRIM31 is upregulated in hepatocellular carcinoma and promotes disease progression by inducing ubiquitination of TSC1-TSC2 complex. *Oncogene* 2018;37:478-88.
 23. Fong KW, Zhao JC, Song B, et al. TRIM28 protects TRIM24 from SPOP-mediated degradation and promotes prostate cancer progression. *Nat Commun* 2018;9:5007.
 24. Zhu H, Chen Y, Zhang J, et al. Knockdown of TRIM37 Promotes Apoptosis and Suppresses Tumor Growth in Gastric Cancer by Inactivation of the ERK1/2 Pathway. *Onco Targets Ther* 2020;13:5479-91.
 25. Chen JX, Xu D, Cao JW, et al. TRIM47 promotes malignant progression of renal cell carcinoma by degrading P53 through ubiquitination. *Cancer Cell Int* 2021;21:129.
 26. Naveed M, Ali A, Sheikh N, et al. Expression of TRIM22 mRNA in chronic hepatitis C patients treated with direct-acting antiviral drugs. *APMIS* 2020;128:326-34.
 27. Zhou Z, Gao W, Yuan B, et al. TRIM22 inhibits the proliferation of gastric cancer cells through the Smad2 protein. *Cell Death Discov* 2021;7:234.
 28. Liu L, Zhou XM, Yang FF, et al. TRIM22 confers poor prognosis and promotes epithelial-mesenchymal transition through regulation of AKT/GSK3 β / β -catenin signaling in non-small cell lung cancer. *Oncotarget* 2017;8:62069-80.
 29. Li L, Qi Y, Ma X, et al. TRIM22 knockdown suppresses chronic myeloid leukemia via inhibiting PI3K/Akt/mTOR signaling pathway. *Cell Biol Int* 2018;42:1192-9.
 30. Hu MM, Shu HB. Multifaceted roles of TRIM38 in innate immune and inflammatory responses. *Cell Mol Immunol* 2017;14:331-8.
 31. Hu MM, Xie XQ, Yang Q, et al. TRIM38 Negatively Regulates TLR3/4-Mediated Innate Immune and Inflammatory Responses by Two Sequential and Distinct Mechanisms. *J Immunol* 2015;195:4415-25.
 32. Park HH, Kim HR, Park SY, et al. RIPK3 activation induces TRIM28 derepression in cancer cells and enhances the anti-tumor microenvironment. *Mol Cancer* 2021;20:107.
 33. Liu L, Xiao L, Liang X, et al. TRIM28 knockdown increases sensitivity to etoposide by upregulating E2F1 in non-small cell lung cancer. *Oncol Rep* 2017;37:3597-605.
 34. Tan G, Xie B, Yu N, et al. TRIM37 overexpression is associated with chemoresistance in hepatocellular carcinoma via activating the AKT signaling pathway. *Int J Clin Oncol* 2021;26:532-42.
 35. Liang Q, Tang C, Tang M, et al. TRIM47 is up-regulated in colorectal cancer, promoting ubiquitination and degradation of SMAD4. *J Exp Clin Cancer Res* 2019;38:159.
 36. Yang C, Huang X, Li Y, et al. Prognosis and personalized treatment prediction in TP53-mutant hepatocellular carcinoma: an in silico strategy towards precision oncology. *Brief Bioinform* 2021;22:bbaa164.
 37. Huo J, Wu L, Zang Y. Construction and Validation of a Reliable Six-Gene Prognostic Signature Based on the TP53 Alteration for Hepatocellular Carcinoma. *Front Oncol* 2021;11:618976.
 38. Liu Z, Zhang Y, Shi C, et al. A novel immune classification reveals distinct immune escape mechanism and genomic alterations: implications for immunotherapy in hepatocellular carcinoma. *J Transl Med* 2021;19:5.
 39. Khemlina G, Ikeda S, Kurzrock R. The biology of Hepatocellular carcinoma: implications for genomic and immune therapies. *Mol Cancer* 2017;16:149.
 40. Yin L, Zhou L, Xu R. Identification of Tumor Mutation Burden and Immune Infiltrates in Hepatocellular Carcinoma Based on Multi-Omics Analysis. *Front Mol Biosci* 2020;7:599142.
- (English Language Editor: A. Muijlwijk)

Cite this article as: Cao J, Su B, Peng R, Tang H, Tu D, Tang Y, Zhou J, Jiang G, Jin S, Wang Q, Wang A, Liu R, Deng Q, Zhang C, Bai D. Bioinformatics analysis of immune infiltrates and tripartite motif (*TRIM*) family genes in hepatocellular carcinoma. *J Gastrointest Oncol* 2022;13(4):1942-1958. doi: 10.21037/jgo-22-619